THE ASTROPHYSICAL JOURNAL, 494:715–723, 1998 February 20

RATES OF ENERGY GAIN AND LOSS IN THE CIRCUMSTELLAR ENVELOPES OF Be STARS: THE POECKERT-MARLBOROUGH MODEL

C. E. MILLAR[1,2] AND J. M. MARLBOROUGH[1,3]

Received 1997 May 15; accepted 1997 September 30

ABSTRACT

We have determined the kinetic temperature of the electron gas as a function of position in the circumstellar envelopes of early Be stars for the model developed by Poeckert & Marlborough. The rates of energy gain and loss due to photoionization, radiative recombination, collisional transitions between bound levels, free-free emission, and free-free absorption were calculated at a set of grid points in a meridional plane. If the temperature assumed is correct, the ratio of energy gain to energy loss should be exactly 1 at all points in the envelope. Our investigation demonstrates that the choice of a constant temperature of 20,000 K was a reasonable first-order approximation. More importantly, we have also determined the temperature that corresponds to equal rates of energy gain and loss at each grid point throughout the envelope. These temperatures represent a self-consistent solution of the equation of energy conservation.

Subject headings: circumstellar matter — stars: early-type — stars: emission-line, Be

1. INTRODUCTION

Be stars are rapidly rotating, early-type stars on or near the main sequence. These stars exhibit hydrogen emission lines at optical and infrared wavelengths and frequently emission from singly ionized metals as well. The hydrogen emission lines arise by recombination in ionized circumstellar material, and are frequently variable on a wide range of timescales (Underhill & Doazan 1982). Further discussion of the emission lines and the spectra of Be stars in other wavelength regions can be found in review articles of Balona et al. (1994), Slettebak & Snow (1987), and references therein.

It has long been accepted that the circumstellar emitting region of Be stars is not spherically symmetric (Coyne & McLean 1981). This expectation has recently been confirmed by direct imaging (see Dougherty & Taylor 1992; Quirrenbach et al. 1993; Stee et al. 1995); the circumstellar region is much more disk-like than spherical. In addition, recent results of Quirrenbach et al. (1997) and Wood et al. (1997) indicate that the disks around some Be stars are quite thin; for example, Wood, Bjorkman, & Bjorkman (1997) find a disk half-opening angle of 2°.5 for ζ Tauri.

A complete hydrodynamical treatment of the structure and dynamics of this disk-like circumstellar envelope is, however, an overwhelmingly complex problem. Because of the complexity of the equations, initial models were more or less ad hoc (Marlborough 1976, 1987). More recently, these ad hoc models have received some theoretical support. Bjorkman & Cassinelli (1993) have shown that under certain restrictive assumptions, a radiation driven wind from the polar regions of a rapidly rotating star is deflected toward the equatorial plane. The part of the radiation-driven wind near the equatorial plane is compressed, and this compressed, less rapidly expanding wind qualitatively resembles the ad hoc models. Owocki, Cranmer, & Blondin (1994) confirmed this general picture by numerical calculations. Recently, however, some doubts have arisen; Owocki, Cranmer, & Gayley (1996) suggest that a wind-compressed disk may not be formed if the stellar wind is a strong-line, radiation-driven wind of the CAK type (see Castor, Abbott, & Klein 1975). Lamers & Pauldrach (1991) have suggested that the existence of these disks in general might be due to the bistability mechanism of radiation-driven winds. However, they further emphasized that this mechanism is unlikely to be dominant in classical Be stars, unless the equatorial mass loss rate is larger than commonly accepted.

An additional simplification, almost always made, has been to bypass the equation for the conservation of energy and instead assume a value, or a simple functional form, for the kinetic temperature of the circumstellar matter. Klein & Castor (1978) considered the winds of Of stars and showed that, since radiative terms dominate in the equation for the conservation of energy, the temperature of the circumstellar matter is determined almost completely by the condition of radiative equilibrium. For these spherically symmetric winds, the electron temperature is approximately constant with distance from the star, and slightly smaller than the stellar effective temperature. More recently, Drew (1989) extended the work of Klein & Castor (1978) to include the most abundant heavy elements and found that the electron temperature decreased gradually with increasing radial distance from the star. For disk-like winds, however, the kinetic temperature may vary with position in the disk in a more complex way, because of the two-dimensional character of the density distribution of the circumstellar matter.

In recent years, there have been several claims that the energy emitted in lines and continua from the circumstellar envelopes of Be stars is inconsistent with that present in the Lyman and/or Lyman plus Balmer continua of the central star. Ashok et al. (1984) were among the first to make such a claim. However, van Kerwijk, Waters, & Marlborough (1995) noted that this conclusion was incorrect because Ashok et al. (1984) had neglected to include the effect of optical depths on line emission. Apparao & Tarafdar (1987) have also argued that an additional source of high-energy photons is needed to account for the observed Balmer line emission, especially for the cooler Be stars. S. P. Tarafdar (1994, 1995, private communication) has also questioned

[1] University of Western Ontario, Department of Physics and Astronomy, London, Ontario, Canada N6A 3K7.
[2] cmillar@io.astro.uwo.ca.
[3] marlboro@titan.astro.uwo.ca.

TABLE 1

DENSITY GRID

r	z	$n = 1$	$n = 2s$	$n = 2p$	$n = 3$	$n = 4$	$n = e$
1.00.....	0.00	3.9E09	1.9E06	5.7E06	4.0E06	4.8E06	3.3E13
	0.03	5.8E08	2.5E05	7.6E05	6.0E05	7.2E05	1.3E13
	0.07	2.1E05	8.4E01	2.5E02	2.5E02	2.5E02	2.3E11
	0.10	2.9E02	7.2E−2	3.5E−3	1.3E−2	2.3E−2	6.4E09
1.05.....	0.00	6.4E10	6.4E07	1.9E08	1.2E08	1.5E08	2.5E13
	0.04	1.5E10	5.3E05	1.6E06	6.3E05	7.3E05	7.8E12
	0.08	2.7E06	6.6E02	2.0E03	1.9E03	2.1E03	5.3E11
	0.12	1.6E03	2.3E−1	1.2E−2	4.3E−2	7.9E−2	1.2E10
1.15.....	0.00	1.3E13	5.7E10	1.7E11	1.1E11	1.3E11	2.6E12
	0.05	1.5E10	1.5E06	4.4E06	2.0E06	2.4E06	7.8E12
	0.10	7.0E06	1.3E03	4.0E03	3.7E03	4.1E03	5.8E11
	0.15	7.8E03	6.0E−1	3.9E−2	1.3E−1	2.3E−1	2.0E10
1.25.....	0.00	1.1E13	6.8E10	2.0E11	3.4E10	3.0E10	8.3E01
	0.06	1.2E10	1.2E06	3.7E06	1.7E06	2.1E06	5.9E12
	0.13	1.1E07	1.6E03	4.9E03	4.4E03	4.9E03	5.4E11
	0.19	1.5E04	8.0E−1	5.7E−2	1.8E−1	3.4E−1	2.3E10
1.35.....	0.00	8.3E12	3.5E10	1.1E11	8.0E10	1.1E11	6.8E02
	0.07	9.1E09	9.6E05	2.9E06	1.3E06	1.6E06	4.6E12
	0.15	1.7E07	1.7E03	5.0E03	4.4E03	5.0E03	4.8E11
	0.22	2.0E04	8.8E−1	6.3E−2	2.0E−1	3.7E−1	2.4E10
1.50.....	0.00	6.1E12	5.8E09	1.8E10	1.0E10	1.2E10	6.5E01
	0.09	6.6E09	6.6E05	2.0E06	9.1E05	1.1E06	3.3E12
	0.19	3.3E07	1.6E03	4.7E03	4.0E03	4.5E03	3.9E11
	0.28	2.4E04	8.8E−1	5.8E−2	1.8E−1	3.4E−1	2.3E10
1.75.....	0.00	3.6E12	1.5E10	4.4E10	5.2E10	5.3E10	2.4E01
	0.13	3.4E09	2.0E05	6.0E05	2.4E05	2.8E05	1.7E12
	0.23	7.6E08	7.1E03	2.1E04	7.1E03	7.8E03	4.1E11
	0.36	2.5E04	7.4E−1	4.0E−2	1.2E−1	2.3E−1	1.9E10
2.00.....	0.00	2.5E12	2.3E09	6.8E09	1.9E10	3.7E10	1.6E01
	0.14	2.9E09	2.4E05	7.3E05	3.2E05	3.8E05	1.5E12
	0.31	3.1E08	2.1E03	6.3E03	2.4E03	2.6E03	2.1E11
	0.45	2.2E04	6.0E−1	2.6E−2	8.1E−2	1.5E−1	1.5E10
2.30.....	0.00	1.5E12	5.3E08	1.6E09	1.3E09	3.6E10	1.1E00
	0.20	1.5E09	6.4E04	1.9E05	7.3E04	8.4E04	7.5E11
	0.38	2.2E08	1.3E03	3.8E03	1.3E03	1.4E03	1.3E11
	0.56	1.4E04	4.1E−1	1.2E−2	3.7E−2	7.0E−2	1.0E10
2.60.....	0.00	9.8E11	3.8E09	1.2E10	3.9E09	3.8E09	2.5E00
	0.21	1.2E09	5.9E04	1.8E05	6.9E04	8.0E04	5.9E11
	0.45	1.4E08	7.2E02	2.2E03	7.8E02	8.3E02	9.1E10
	0.66	8.7E03	2.8E−1	5.9E−3	1.9E−2	3.5E−2	7.3E09
3.00.....	0.00	5.9E11	2.5E09	7.6E09	4.8E09	5.9E09	6.0E00
	0.25	7.0E08	2.8E04	8.4E04	3.1E04	3.6E04	3.7E11
	0.51	1.4E08	8.7E02	2.6E03	8.8E02	9.5E02	8.1E10
	0.80	5.1E03	1.8E−1	2.6E−3	8.0E−3	1.5E−2	4.8E09
3.75.....	0.00	2.7E11	3.6E08	1.1E09	5.8E09	7.4E09	4.4E−2
	0.34	3.3E08	9.3E03	2.8E04	9.9E03	1.1E04	1.7E11
	0.73	4.0E07	1.9E02	5.6E02	1.0E02	1.9E00	2.8E10
	1.06	2.1E03	9.1E−2	6.8E−4	2.1E−3	4.0E−3	2.5E09
4.50.....	0.00	1.5E11	6.1E08	1.8E09	2.2E09	4.3E09	6.2E−2
	0.42	1.8E08	3.9E03	1.2E04	4.0E03	4.5E03	9.7E10
	0.84	3.4E07	1.8E02	5.5E02	9.8E01	1.3E00	2.2E10
	1.33	1.0E03	5.1E−2	2.3E−4	7.2E−4	1.4E−3	1.4E09
6.00.....	0.00	6.3E10	7.8E07	2.3E08	1.1E08	1.6E08	3.0E−1
	0.58	7.2E07	1.1E03	3.2E03	1.1E03	1.2E03	3.9E10
	1.27	5.3E06	2.3E01	6.9E01	2.5E00	5.9E−2	6.6E09
	1.85	3.3E02	2.0E−2	3.9E−5	1.3E−4	2.4E−4	6.1E08
8.00.....	0.00	2.1E10	1.8E02	2.7E03	8.4E02	1.1E03	3.E−16
	0.81	2.3E07	2.4E02	7.2E02	1.6E02	7.1E−1	1.3E10
	1.74	7.5E05	3.8E00	1.1E01	7.7E−2	5.9E−3	2.2E09
	2.55	6.7E01	6.1E−3	4.4E−6	1.5E−5	2.7E−5	2.0E08
12.00.....	0.00	8.4E06	4.7E−1	1.4E00	7.7E−1	9.5E−1	4.9E09
	1.25	4.9E06	3.2E01	9.5E01	2.6E00	1.4E−2	3.0E09
	2.70	3.7E04	3.6E−1	1.1E00	2.3E−4	3.1E−4	5.3E08
	3.95	8.6E00	1.2E−3	2.5E−7	8.8E−7	1.7E−6	5.1E07

TABLE 1—*Continued*

r	z	$n=1$	$n=2s$	$n=2p$	$n=3$	$n=4$	$n=e$
16.00.....	0.00	3.4E06	4.3E01	1.3E02	6.2E00	7.4E−3	1.9E09
	1.69	1.7E06	7.8E00	2.4E01	1.3E−1	1.7E−3	1.2E09
	3.66	1.8E03	3.5E−2	8.8E−2	2.1E−5	3.3E−5	2.0E08
	5.35	2.3E00	3.9E−4	3.7E−8	1.3E−7	2.5E−7	2.0E07
20.00.....	0.00	1.7E06	1.7E01	5.0E01	9.8E−1	1.4E−3	9.9E08
	2.13	7.9E05	3.2E00	9.6E00	2.1E−2	4.5E−4	6.1E08
	4.62	4.4E02	9.6E−3	1.8E−2	4.8E−6	8.2E−6	1.1E08
	6.75	9.7E−1	1.8E−4	1.0E−8	3.7E−8	7.0E−8	1.0E07
28.00.....	0.00	5.5E05	4.7E00	1.4E01	1.0E−1	2.2E−4	4.1E08
	3.02	3.0E05	1.0E00	3.1E00	2.2E−3	7.8E−5	2.5E08
	6.53	1.0E02	2.5E−3	2.7E−3	7.6E−7	1.4E−6	4.5E07
	9.55	3.4E−1	6.3E−5	1.8E−9	6.6E−9	1.2E−8	4.4E06
36.00.....	0.00	2.4E05	1.6E00	4.9E00	1.5E−2	5.5E−5	2.1E08
	3.90	1.4E05	4.3E−1	1.3E00	1.6E−5	2.1E−5	1.3E08
	8.45	3.9E01	1.0E−3	6.0E−4	1.9E−7	3.6E−7	2.3E07
	12.35	1.5E−1	2.9E−5	5.E−10	1.8E−9	3.3E−9	2.3E06
50.00.....	0.00	1.0E05	6.0E−1	1.8E00	2.4E−3	1.3E−5	1.0E08
	5.45	7.1E04	1.7E−1	5.1E−1	3.5E−6	4.6E−6	6.2E07
	11.80	1.6E01	4.3E−4	1.4E−4	4.4E−8	8.2E−8	1.1E07
	17.25	6.5E−2	1.2E−5	1.E−10	4.E−10	8.E−10	1.1E06
75.00.....	0.00	4.5E04	2.2E−1	6.6E−1	4.1E−4	2.5E−6	4.5E07
	8.21	3.5E04	5.6E−2	1.7E−1	6.1E−7	8.3E−7	2.8E07
	17.79	5.8E00	1.8E−4	3.2E−5	8.5E−9	1.6E−8	4.9E06
	26.00	2.9E−2	5.3E−6	2.E−11	8.E−11	2.E−10	4.8E05

whether the kinetic temperature assumed for the circumstellar matter in the Poeckert-Marlborough (PM) model is too high.

In the remainder of this paper we first test PM's choice of kinetic temperature by evaluating the energy gains and losses as a function of position in the circumstellar matter. Then we determine at each point in the envelope the temperature at which the rates of energy gain and loss are balanced.

2. THE PM MODEL

One of the ad hoc models for Be stars, the so-called PM model, was introduced by Marlborough (1969) and subsequently modified considerably by Poeckert & Marlborough (1978, hereafter PM). In this model, the density of the circumstellar envelope in the equatorial plane at the surface of the star is specified arbitrarily, as is the radial component of velocity in the equatorial plane. The density distribution in the equatorial plane is then determined using the equation of continuity; the density distribution perpendicular to the equatorial plane is assumed to be hydrostatic. Finally, the kinetic temperature of the envelope must be chosen; in the PM model, the temperature was assumed to be constant, although a simple dependence on distance in the equatorial plane could also have been used.

PM produced a detailed model of this kind for the Be star γ Cas (B0 IVe). The stellar mass, radius, effective temperature and log g were chosen to have the values 17 $M_{\odot}$, 10 $R_{\odot}$, 25,000 K, and 3.5, respectively. PM assumed a steady-state, circumstellar envelope that was symmetric about both the rotation axis and the equatorial plane. The circumstellar matter was assumed to have a kinetic temperature of 20,000 K, this choice being qualitatively consistent with Klein & Castor (1978).

The ionization-excitation equilibrium was then determined at various locations in a meridional plane by solving the statistical equilibrium equations for the level populations of hydrogen, using both the assumed kinetic temperature of the gas and the local stellar radiation field; the local radiation field is the local value of the photospheric radiation field reduced for both geometrical and physical dilution. We emphasize that no assumption was made in advance concerning the degree of ionization of the circumstellar envelope. Complete details are given by Marlborough (1969), PM, and references therein. The shortcomings of the PM model are many; they will not all be enumerated here. Details can be found in Wood et al. (1997), van Kerkwijk et al. (1995), Waters & Marlborough (1994), and references therein.

In the course of our investigations, we discovered and corrected a coding error in one of subroutines of the original PM code. This error affected the level populations in regions of the envelope where an assumption that the gas is optically thick in all lines was used. Furthermore, PM's choice of 4 grid points perpendicular to the equatorial plane led to inadequate sampling of the exponential density distribution in this direction; we have increased the number of such points to 20. The corrected level populations at each of the grid points tabulated by PM are given in Table 1. Note that only the populations corresponding to radial distances between 1.50 and 8.00 stellar radii near the equatorial plane have been significantly altered.

3. ENERGY GAINS AND LOSSES OF THE PM MODEL

We assume that the gas dynamical terms in the equation for the conservation of energy are sufficiently small that the gas in the circumstellar envelope can be assumed to be in radiative equilibrium, so that at each point in the envelope the radiative heating and cooling rates balance. Klein & Castor (1978) demonstrated that this assumption was a good one for the rapidly expanding Of star winds that they investigated. In the PM model, the radial component of velocity of the circumstellar matter is considerably smaller and the particle density generally larger than the same

quantities in the Of star winds, so our assumption is expected to be valid at least for the equatorial regions of the circumstellar envelopes of Be stars. It may also be a reasonable assumption for the bulk of the circumstellar envelope.

At any point in the circumstellar envelope, a variety of processes at the microscopic level convert energy in the form of radiation into internal and/or thermal energy of the gas and vice versa. Free electrons in a unit volume of gas gain energy from photoionization, collisional deexcitation of bound levels, and free-free absorption; electrons lose energy by recombination, collisional excitation, and free-free emission.

The PM model requires that a gas temperature be initially specified. We can evaluate the rates of energy conversion, determine their ratio at each grid location and compare this ratio to unity. If by chance the correct temperature were assumed, this ratio would be unity at each location. If the ratio is not unity at a specific grid point, the choice of temperature at that grid point is not correct. An average of this ratio for all grid points permits us to assess the validity of the isothermal envelope temperature of 20,000 K assumed by PM. In addition, by determining this ratio at each grid point considered in the envelope, the temperature at which the rates balance can be determined iteratively at each grid point. In the following subsection, we describe the procedures by which each of these rates of energy conversion was evaluated.

3.1. *Energy Rate Calculations*

The energy gain per electron from photoionization, $E_{n,\infty}$, was determined by multiplying the integrand of the standard integral used to determine the number of photoionizations from level n per unit volume per unit time per particle by $h(\nu - \nu_n)$,

$$E_{n,\infty} = \int_{\nu_n}^{\infty} \frac{c}{h\nu} h(\nu - \nu_n) a_n(\nu) u_\nu \, d\nu \,, \tag{1}$$

where ν_n is the series limiting frequency for photoionization from level n, c is the speed of light, $a_n(\nu)$ is the cross section for photoionization at frequency ν, u_ν is the energy density of radiation at frequency ν, and h is Planck's constant. The same numerical scheme as employed in the PM model to evaluate the photoionization rate was used to evaluate this integral.

The energy emitted as a result of capture of electrons to level n per unit volume per unit time is given by

$$R_{\infty,n} = \frac{4\pi}{c^2} N_e N_+ \left[\frac{g_+}{g_n} \frac{(2\pi m_e kT)^{3/2}}{h^3}\right]^{-1} \exp\left(\frac{I_n}{kT}\right) \times \int_{\nu_n}^{\infty} \nu^2 h(\nu - \nu_n) a_n(\nu) \exp\left(-\frac{h\nu}{kT}\right) d\nu \,, \tag{2}$$

where c is the speed of light, m_e is the mass of the electron, k is the Boltzmann constant, N_e is the number density of free electrons, N_+ is the number density of ions, I_n is the minimum ionization energy from level n, and $a_n(\nu)$ is the cross section for photoionization at frequency ν from level n. A 7 point Gauss-Laguerre integration scheme was used to evaluate this integral.

Radiative excitation of a bound electron followed by collisional deexcitation represents a net energy gain by the electron gas. Conversely, a collisional excitation followed by a radiative deexcitation will result in an energy loss. Therefore, if one knows the population of a particular level, the number density of free electrons, the collisional transitional rates, and the difference in energy between the two levels involved in the transition, then the losses and gains of energy of the electron gas due to transitions between bound levels can easily be calculated. Note that in the PM model, only collisional transitions that involved a change in the principle quantum number of ± 1 were considered. We will consider only these same transitions in this paper.

The energy loss by free-free emission or bremsstrahlung can easily be calculated using the standard expression (Osterbrock 1974). Alternatively, a free electron may absorb a photon and make a transition to a higher state, which increases the energy of the gas; this is free-free absorption or inverse bremsstrahlung (Tucker 1975). These free-free terms are not in general expected to be dominant contributors to energy gains and losses. However, in portions of the envelope where densities are lower, free-free emission does become a factor in energy loss, so these terms have been included for completeness.

4. RESULTS

The equations used to determine the energy losses and gains depend explicitly in a nonlinear way on temperature, and have an additional complex, implicit dependence on temperature through the level populations. If the assumed temperature of the envelope at a given grid point were exactly correct, the rate of energy gain per unit volume divided by the rate of energy loss at that location would be exactly 1. In considering the original isothermal case, we have used the ab initio assumption for the temperature of 20,000 K made by PM. A simple global average of the ratio of energy gain to loss for this 20,000 K, isothermal model is 0.6 ± 0.3 (1 σ); a density-weighted average of the same ratio is 0.76 ± 0.02 (1 σ). The density-weighted average is dominated by regions of the envelope near both the star and the equatorial plane, where densities are high. We conclude that the temperature assumed by PM was a reasonable first-order approximation.

In order to determine the temperature corresponding to equal rates of energy gain and loss, the PM code was modified to permit the electron temperature to be a function of position. An initial guess for the temperature grid was determined in the following manner. The ratio of the rate of energy gain to loss was computed at each grid point for isothermal model envelopes characterized by a specific choice for the kinetic temperature of the gas. This process was then repeated for a range of kinetic temperatures. Therefore, at each grid point a series of such ratios was obtained; each ratio corresponds to a particular constant-temperature envelope. At each grid point, interpolation among the set of energy ratios yielded the temperature required for equal rates of energy gain and loss. Subsequently, this temperature grid was used as an initial guess for the temperature. Then the ionization-excitation program was run, level populations were recalculated, and a new energy ratio was determined at each grid position. The temperature was readjusted at individual grid points and the ionization-excitation program was rerun until the ratio of energy gain to loss at each grid point differed from unity by less than some prescribed amount. Varying the temperature at a grid point changed the ratio of gain to loss by an amount that depended on the processes that were dominant at that particular position. Experience allowed one to

determine whether to increase or decrease the temperature at a particular grid point, depending on the value of the ratio there. Temperature adjustments were made in steps of at least 500 K. This iterative process was repeated until the standard deviation of the energy ratios in the final solution was ≤ 0.01, for consistency. However, individual temperatures are certainly not this accurate. The error of the level populations is at least 5%, due to the manner in which they are determined. We have not attempted to assign absolute errors to the predicted temperatures because of the uncertainties in many of the parameters used. Nevertheless, the resulting temperature grid does represent a consistent solution for which the equation of energy conservation is satisfied.

The number of grid points in the z-direction, each of which is referred to by its J value, with $J = 1$ in the equatorial plane, was increased from four equally spaced points in the original PM model to 20 grid points, spaced unequally in order to better sample the exponential density decrease in the PM model perpendicular to the equatorial plane. Thus, there are 480 grid points, 20 J values for each of the 24 ϖ values. At positions in the envelope corresponding to $J = 20$ ($J = 4$ in the PM model), it was assumed that there was no material above these locations. This assumption is unphysical, since there will certainly be some material beyond these positions. Therefore, the grid points corresponding to $J = 20$ were excluded from the final analysis.

A simple global average of the energy ratios corresponding to the set of final temperatures is 1.00 ± 0.01 (1 σ). This demonstrates that the rates of energy gain and energy loss are balanced throughout the envelope. A density-weighted average of the energy ratios corresponding to the set of final temperatures is 1.01 ± 0.01 (1 σ). This result is dominated by the energy ratios in the equatorial plane, where densities are high. See Figure 1 for a graph of temperature versus radial position in the equatorial plane, at the upper edge, and at an intermediate position. The portion of the envelope nearest to the star has been expanded in the lower part of the figure, to resolve temperature variations more easily. The $J = 19$ position varies from a height of 0.10 stellar radii above the equatorial plane at the surface of the star to a height of 34.40 stellar radii at a radial distance of 100 stellar radii. The $J = 6$ position, referred to in Figure 1, corresponds to a height of 0.03 stellar radii at the stellar surface, a height of 1.19 stellar radii at a radial distance of 12 stellar radii, and increases to a height of 10.4 stellar radii at a radial distance of 100 stellar radii; these positions correspond to scale heights of 0.9, 0.4, and 0.4, respectively. The temperature curves are relatively flat, except for distances within 6 stellar radii of the star's surface. It is apparent that temperatures within the envelope are strongly dependent on the height above the equatorial plane.

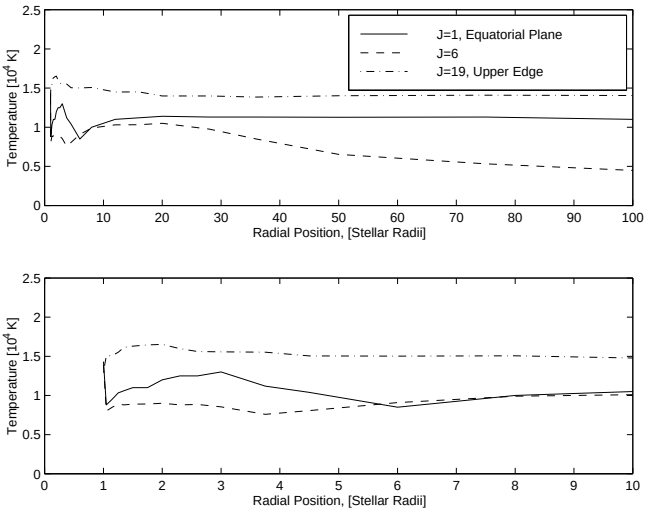

FIG. 1.—Temperature for which the energy gain balances the energy loss as a function of distance from the rotation axis for three locations in the circumstellar envelope: the equatorial plane ($J = 1$), an intermediate location ($J = 6$), and the upper edge ($J = 19$).

It should be emphasized that there is no monotonic increase in temperature between the equatorial plane and the upper edge of the envelope. In the upper portions of the envelope, energy gains and losses are dominated by radiative processes, in particular photoionization and radiative recombination. Along the equatorial plane, collisional processes dominate the energy terms out to a distance of approximately 4.5 stellar radii. In fact, the most conspicuous feature in Figure 1 is a temperature increase and subsequent decrease of approximately 5000 K in the equatorial plane between 1 and 5 stellar radii, where collisional processes dominate. Between 4.5 and 8 stellar radii, collisional energy terms are the same order of magnitude as the radiative terms. At increasing heights above the equatorial plane, the temperature structure is quite complicated because collisional terms gradually decrease in importance as the particle number density decreases. Generally, the temperature decreases with increasing height above the equatorial plane because the energy density of radiation remains low and collisions become less important as number densities decrease exponentially (see Fig. 1, $J = 6$). Farther from the equatorial plane, the temperature begins to increase as energy densities increase, since the envelope gradually becomes optically thin in the continuum.

The envelope is almost completely ionized everywhere. However, over a small region in the equatorial plane near the star, the degree of ionization is reduced. At a radial distance of 1.05 stellar radii up to a height above the plane of 0.05 stellar radii and out to 2.6 stellar radii up to a height of 0.03 stellar radii, the degree of ionization varies between 45% and 75%. In this region, the temperature is approximately 15,000 K; see Figure 1. The original PM model assumed a constant temperature of 20,000 K and a gas that was largely ionized. In the corrected PM model, between radial distances of 1.15 and 8.0 stellar radii up to a maximum height of 0.14 stellar radii from the equatorial plane, the envelope is largely neutral (see Table 1). The cause of this lower degree of ionization in a larger region and at a higher temperature in the corrected PM model as compared to the variable temperature model is straightforward. The collisional transition probabilities between bound levels are strongly sensitive to temperature. At higher temperatures, collisions populate the upper levels more effectively. This results in larger column densities at frequencies corresponding to photoionization from these upper levels, and these large column densities decrease the energy density of stellar radiation reaching these locations. Consequently, the probability of photoionization per particle is substantially reduced, and the envelope becomes neutral. The variation in the degree of ionization between these models, which have a difference of only 5000 K in temperature in this particular region of the envelope,

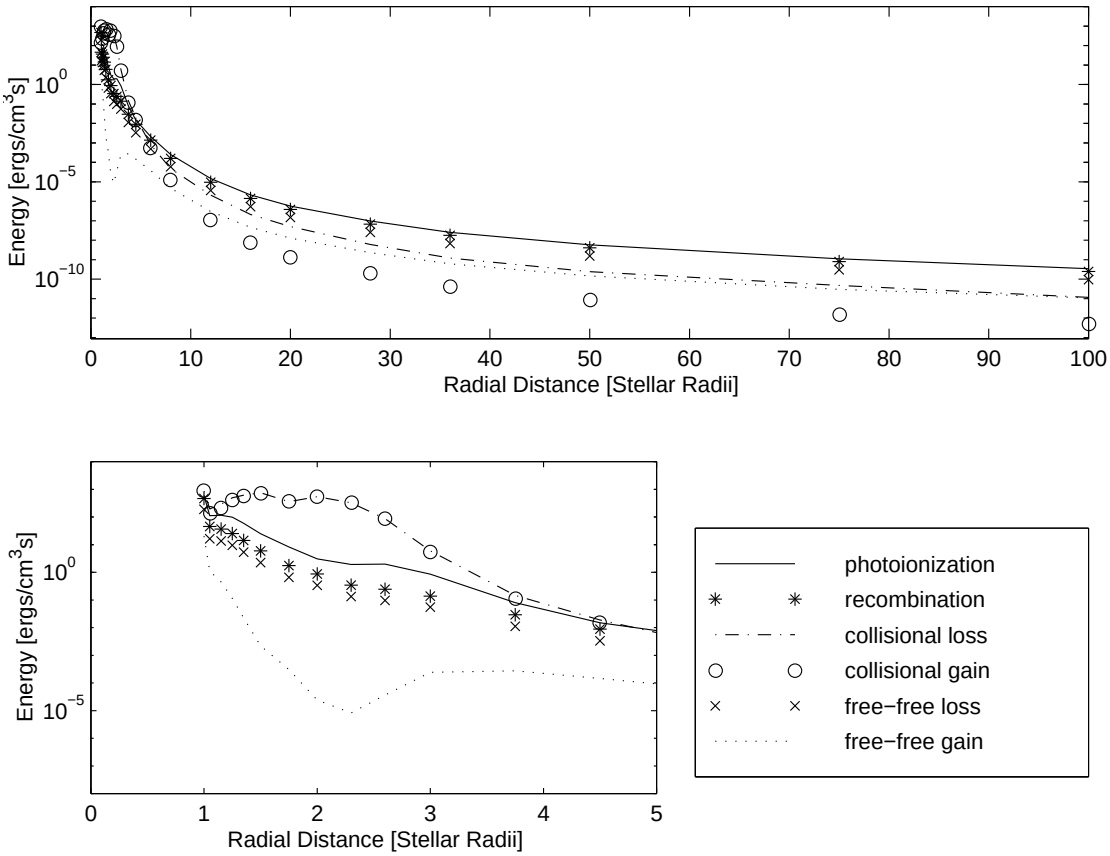

FIG. 2.—The sources of energy gain and loss along the equatorial plane ($J = 1$)

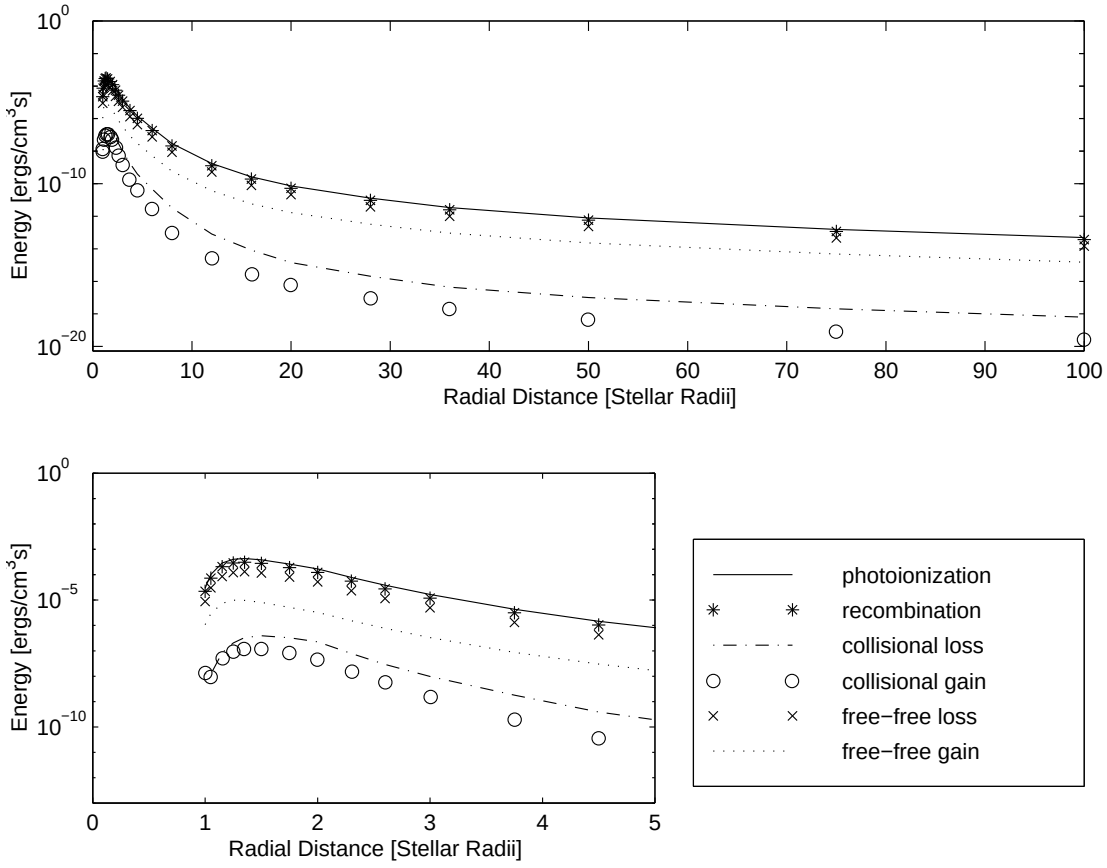

FIG. 3.—Same as Fig. 2, for the upper envelope ($J = 19$)

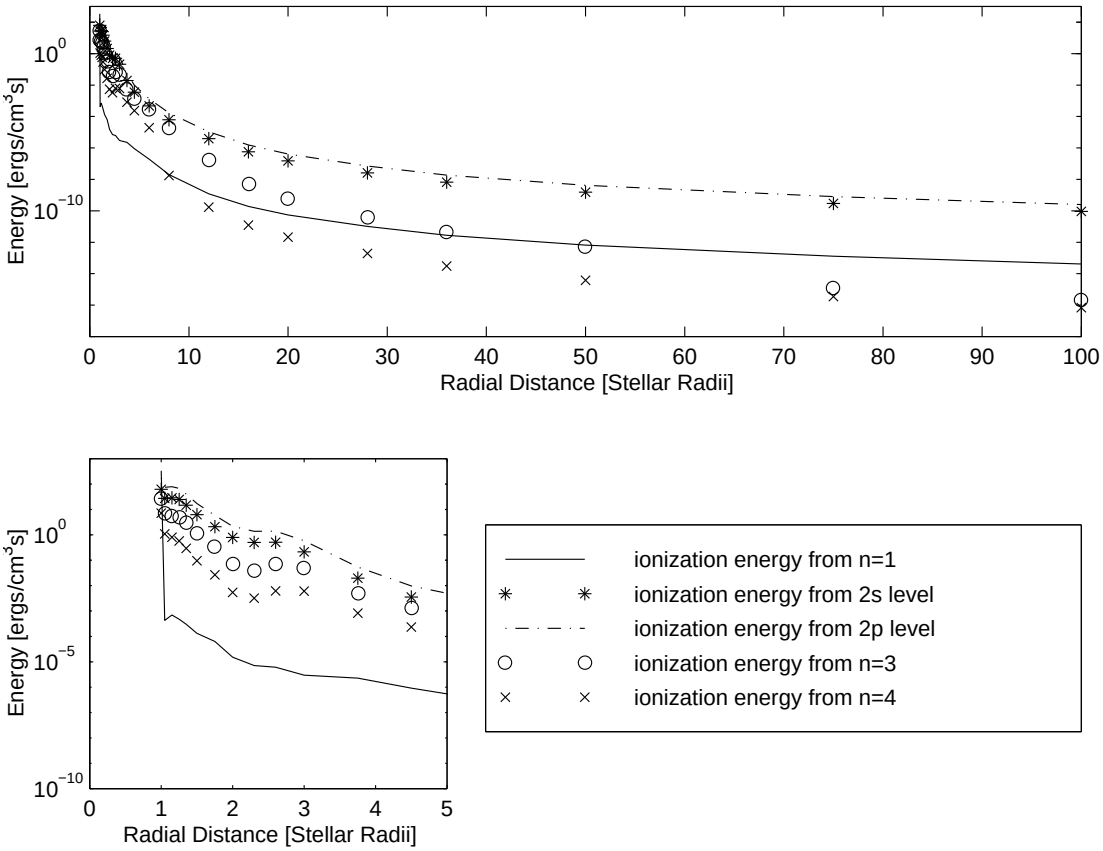

FIG. 4.—Contribution of ionization energy from levels $n = 1, 2s, 2p, 3$, and 4 for the equatorial plane ($J = 1$)

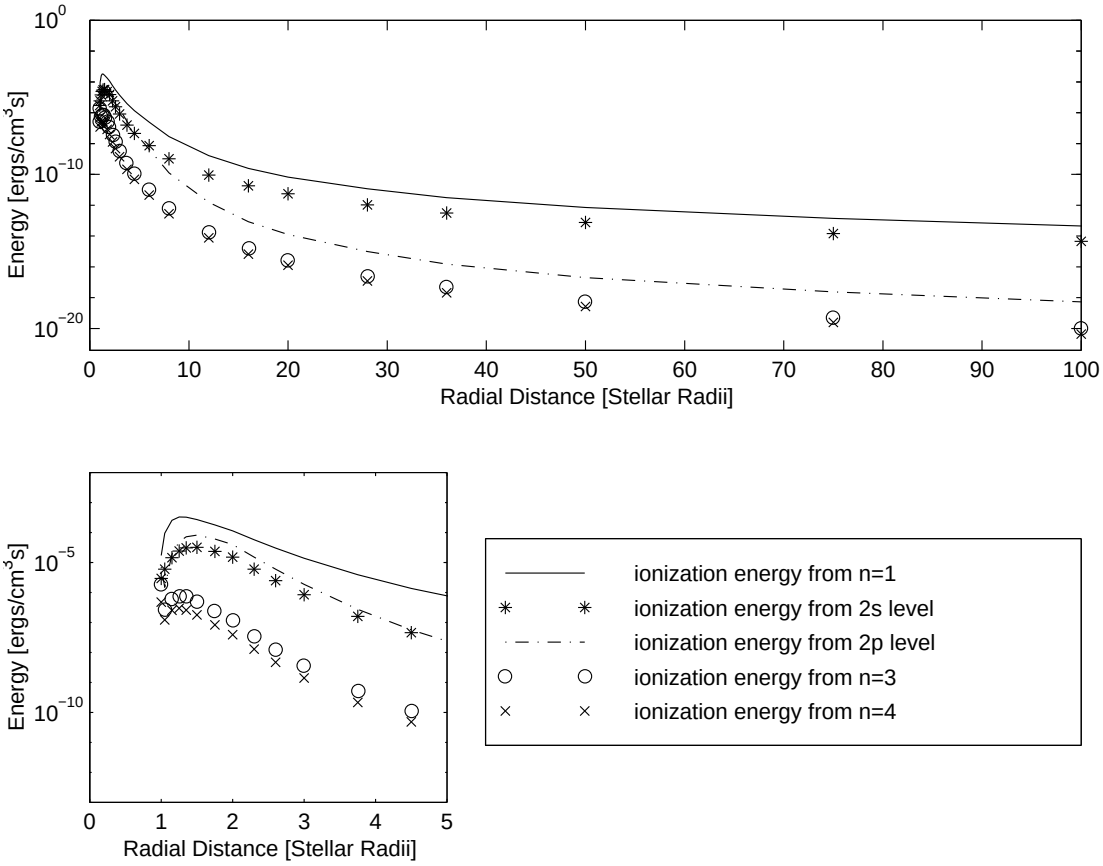

FIG. 5.—Same as Fig. 4, for the upper envelope ($J = 19$)

further illustrates the need to have a self-consistent solution for which the equation of energy conservation is satisfied.

In the equatorial plane, at distances greater than 5 stellar radii, photoionization and radiative recombination are the dominant energy terms. At distances within 5 stellar radii, collisional processes dominate the energy terms. Collisions dominate where number densities are large. In the equatorial plane near the star number, densities are on the order of 10^{13} cm^{-3}. Figure 2 shows the relative importance of the energy terms in the equatorial plane. Beyond a distance of 4.5 stellar radii, the collisional terms cease to be the dominant energy terms. In fact, even within 8 stellar radii, at heights greater than approximately 0.6 stellar radii above the equatorial plane, radiative terms dominate. Figure 3 shows the relative importance of the energy terms along the upper edge of the envelope. As expected, radiative terms dominate at all radial distances.

Figures 4 and 5 show the relative importance of photoionization from levels $n = 1$, $2s$, $2p$, 3, and 4 along the equatorial plane and along the upper edge of the envelope. In the equatorial plane near the star, the densities are high and the envelope is optically thick in line radiation. Collisional processes and scattered line radiation result in increased populations above the ground state, and radiation is available in the Balmer and longer wavelength continua to ionize the atoms. Consequently, photoionization from the $2p$ and $n = 3$ levels contributes the most energy input to the envelope in the equatorial plane. Photoionization from $n = 1$ is substantially reduced between radial distances of 1.05 and 8.0 stellar radii, where the envelope is not completely ionized. Farther from the equatorial plane, the envelope more closely resembles a nebula, with most of the ionization coming from the ground state.

5. DISCUSSION

It is evident from a consideration of either the simple global average or the density-weighted average of the ratio of energy gain to loss that PM's choice of a constant kinetic temperature of 20,000 K was a reasonable first-order approximation for the temperature of the circumstellar envelope of γ Cas. Nevertheless, as shown in Figure 1, the kinetic temperature does have a moderately strong positional dependence, so that the assumption of a constant kinetic temperature is at best a zeroth-order approximation. More realistic models for the circumstellar matter around Be stars and similar objects will of necessity have to include the dependence of kinetic temperature on position in the envelope. The modified PM model described in this paper represents the first such approach of which we are aware.

Several assumptions were used in evaluating the ionization-excitation equilibrium in the PM model. We review these here to allow the reader to judge the appropriateness or otherwise of the approximations used and therefore the accuracy of the temperature structure of the envelope we have obtained. The procedure used to obtain the ionization-excitation conditions has been described by Marlborough (1969) and PM. Several simplifying assumptions were made, which affect the determination of the kinetic temperature.

1. The contribution of the diffuse radiation field to the local continuum background was neglected in evaluating the photoionization rates from each bound level. By neglecting the diffuse radiation field, we have underestimated both the degree of ionization and the local electron temperature, since the capture of a free electron to the ground state, for example, yields a Lyman continuum photon that can subsequently photoionize a hydrogen atom and, more importantly, heat the gas. Inclusion of the diffuse field will have a more significant effect where the gas is cooler and has a lower degree of ionization, specifically, in those parts of the envelope near the equatorial plane and between 1 and 3 stellar radii from the surface of the star. One expects both the degree of ionization and the temperature of the gas in this region of the envelope to be somewhat higher than our predictions when the diffuse radiation field is included.

2. Only collisional transitions between levels n and $n \pm 1$ were included in the statistical equilibrium equations. This simplification is satisfactory for collisional excitations because the increasing energy threshold reduces the importance of transitions from n to $n + 2$, $n + 3$, etc., compared to the transition n to $n + 1$. A similar simplification is appropriate for collisional deexcitation, because the transition n to $n - 1$ has a higher rate coefficient than n to $n - 2$, etc.

3. A simple approximation was used to evaluate the local energy density of line radiation; this is described in detail by Marlborough (1969). Essentially, this procedure assumes that the energy density of radiation in each line, or, equivalently, the level populations including the effects of the local radiation field in the lines, can be obtained using the local ionization-excitation equilibrium, assuming that a particular series of lines is either optically thick or optically thin, together with the optical depth in line radiation along a path parallel to the rotation axis from the grid point at which the ionization-excitation conditions are being determined to the upper boundary of the envelope. This approach avoids the need to determine the constant velocity surfaces in the rotating, expanding wind, which are required for the Sobolev approximation. The justification for this approximation is the degree to which the PM model satisfactorily reproduced the observational data for γ Cas.

Our investigation has shown that it is possible, given a background density and velocity distribution for the circumstellar envelope, to determine self-consistently both the ionization-excitation equilibrium and the electron temperature distribution as a function of position in the circumstellar envelope. Therefore, we have eliminated the need to arbitrarily assume the kinetic temperature of the gas in the circumstellar envelope.

The variation of the kinetic temperature with position may produce ionization gradients within the circumstellar envelope. In the case of an early B star, for example, for which the PM model may be a reasonable approximation for the structure of the circumstellar envelope, Fe II might be the dominant stage of ionization of iron in the cooler parts, with Fe III dominant in the hotter parts. If this possibility is confirmed, metal lines from different stages of ionization may prove to be valuable probes of the physical conditions in the circumstellar regions of the hotter Be stars. This might also help to resolve the controversy concerning the location of and the electron number density within the region where shell lines form (Hubert 1994).

We are considering extending this analysis to the disk model (Waters 1986; Waters, Coté, & Lamers 1987) in a subsequent paper. The results of these analyses will be used to construct an improved model. These improvements will

include changes to the density distribution above the equatorial plane and flexibility to allow the upper edge of the envelope to vary in shape.

We thank K. M. V. Apparao, and in particular the late S. P. Tarafdar, whose questions and comments stimulated us to carry out this exercise. We also thank the referee, Karen Bjorkman, whose constructive comments and suggestions helped us to improve the paper. This research was supported in part by NSERC, the Natural Sciences and Engineering Research Council of Canada. C. E. M. acknowledges financial support from an NSERC postgraduate scholarship.

REFERENCES

Apparao, K. M. V., & Tarafdar, S. P. 1987, ApJ, 322, 976
Ashok, N. M., Bhatt, H. C., Kulkarni, P. V., & Joshi, S. C. 1984, MNRAS, 211, 471
Balona, L. A., Henrichs, H. F., & Le Contel, J. M., ed. 1994, IAU Symp. 162, Pulsation, Rotation and Mass Loss in Early-Type Stars (Dordrecht: Reidel)
Bjorkman, J. E., & Cassinelli, J. P. 1993, ApJ, 409, 429
Castor, J. I., Abbott, D. C., & Klein, R. I. 1975, ApJ, 195, 157
Coyne, G. V., & McLean, I. S. 1982, in IAU Symp. 98, Be Stars, ed. M. Jaschek & H.-G. Groth (Dordrecht: Reidel), 77
Dougherty, S. M., & Taylor, A. R. 1992, Nature 359, 808
Drew, J. E. 1989, ApJS, 71, 267
Hubert, A. M. 1994, in IAU Symp. 162, Pulsation, Rotation and Mass Loss in Early-Type Stars, ed. L. A. Balona, H. F. Henrichs, & J. M. Le Contel (Dordrecht: Reidel), 341
Klein, R. I., & Castor, J. I. 1978, ApJ, 220, 902
Lamers, H. J. G. L. M., & Pauldrach, A. W. A. 1991, A&A, 244, L5
Marlborough, J. M. 1969, ApJ, 156, 135
———. 1976, in IAU Symp. 70, Be and Shell Stars, ed. A. Slettebak (Dordrecht: Reidel), 335
———. 1987, in IAU Symp. 92, Physics of Be Stars, ed. A. Slettebak & T. P. Snow (Cambridge: Cambridge Univ. Press), 316
Osterbrock D. E. 1974, Astrophysics of Gaseous Nebulae (New York: Freeman)
Owocki, S., Cranmer, S. R., & Blondin, J. M. 1994, ApJ, 424, 887
Owocki, S., Cranmer, S. R., & Gayley, K. G. 1996, ApJ, 472, L115
Poeckert, R., & Marlborough, J. M. 1978, ApJ, 220, 940 (PM)
Quirrenbach, A., Bjorkman, K. S., Bjorkman, J. E., Hummel, C. A., Buscher, D. F., Armstrong, J. T., Mozurkewich, D., Elias, N. M., II, & Babler, B. L. 1997, ApJ, 479, 477
Quirrenbach, A., Hummel, D. F., Buscher, J. T., Armstrong, D., Mozurkewich, D., & Elias, N. M., II. 1993, ApJ, 416, L25
Slettebak, A., & Snow, T. P. 1987, IAU Colloq. 92, Physics of Be Stars, (Cambridge: Cambridge Univ. Press)
Stee, Ph., de Araujo, F. X., Vakili, F., Mourard, D., Arnold, L., Bonneau, D., Morand, F., & Tallon-Bosc, I. 1995, A&A, 300, 219
Tucker, W. H. 1975, Radiation Processes in Astrophysics (Cambridge: M.I.T. Press)
Underhill, A. B., & Doazan, V. 1982, B Stars with and without Emission Lines (NASA SP-465)
van Kerwijk, M. H., Waters, L. B. F. M., & Marlborough, J. M. 1995, A&A, 300, 259
Waters, L. B. F. M. 1986, A&A, 159, L1
Waters, L. B. F. M., Coté, J., & Lamers, H. J. G. L. M. 1987, A&A, 185, 206
Waters, L. B. F. M., & Marlborough, J. M. 1994, in IAU Symp. 162, Pulsation, Rotation and Mass Loss in Early-Type Stars, ed. L. A. Balona, H. F. Henrichs, & J. M. Le Contel (Dordrecht: Reidel), 399
Wood, K., Bjorkman, K. S., & Bjorkman, J. E. 1997, ApJ, 477, 926